Robotica (2015) volume 33, pp. 314–331. © Cambridge University Press 2014
doi:10.1017/S0263574714000356

Kinematic modeling and control for human-robot cooperation considering different interaction roles

B. V. Adorno†*, A. P. L. Bó‡ and P. Fraisse§

†*Department of Electrical Engineering, Universidade Federal de Minas Gerais, Av. Antônio Carlos 6627, CEP 31270-010, Belo Horizonte, MG, Brazil*
‡*Universidade de Brasília, LARA, Caixa Postal 4386, 70919-970 Brasília-DF, Brazil*
§*Université Montpellier 2, LIRMM, 161 rue Ada, 34095 Montpellier, France*

(Accepted February 2, 2014. First published online: February 28, 2014)

SUMMARY
This paper presents a novel approach for the description of physical human-robot interaction (pHRI) tasks that involve two-arm coordination, and where tasks are described by the relative pose between the human hand and the robot hand. We develop a unified kinematic model that takes into account the human-robot system from a holistic point of view, and we also propose a kinematic control strategy for pHRI that comprises different levels of shared autonomy. Since the kinematic model takes into account the complete human-robot interaction system and the kinematic control law is closed loop at the interaction level, the kinematic constraints of the task are enforced during its execution. Experiments are performed in order to validate the proposed approach, including a particular case where the robot controls the human arm by means of functional electrical stimulation (FES), which may potentially provide useful solutions for the interaction between assistant robots and impaired individuals (e.g., quadriplegics and hemiplegics).

KEYWORDS: Physical human-robot interaction (pHRI); Functional electrical stimulation (FES); Kinematic modeling and control for pHRI.

1. Introduction

There is a growing interest in developing robotics systems capable of sharing its workspace along with humans, or even deliberately establishing physical contact with the user. Indeed, there is an increasing social demand for the introduction of robots in human environments, where they may assist in the performance of tasks not taken into account by currently available robotic systems, such as assisting the physically impaired and the elderly.[1] From a technological perspective, the research in pHRI has been supported by advances in robot control, actuator design, and materials technology,[2] since human-friendly robots must incorporate different features for an effective pHRI, such as guaranteed safety and adequate information exchange between human and robot.

A convenient classification of pHRI tasks is based on the level of autonomy assumed by the robot and the corresponding degree of intervention required for the human.[3,4] On the one hand, there are interactions where the human must teleoperate the robot, possibly by directly controlling each available degree of freedom (DOF). On the other hand, there are other applications where the robot has an increased level of autonomy, requiring thus a reduced cognitive effort from the human, who acts mostly as a supervisor. Between these two extreme cases there are several applications where a varying degree of shared autonomy is assumed by the human and the robot, which may actually lead to the establishment of different interaction roles within the task execution.

Another important feature related to pHRI is associated to the interpersonal distance between human and robot. There may be, for instance, situations where human and robot are not collocated, but also those scenarios where human and robot are sharing the same workspace, possibly establishing physical contact. Within the class of applications where human and robot are collocated, there

* Corresponding author. E-mail: adorno@ufmg.br

are different tasks where the interaction force between robot and human and possibly between human/robot and manipulated object is of major importance. For instance, in the context of cooperative carrying, Takubo *et al.* (2012)[5] developed an impedance controller enabling the operator to transport a large object analogously to the operation of a wheelbarrow, simplifying the cooperative handling, whereas Mortl *et al.* (2012)[6] proposed a role allocation policy in order to distribute the carrying effort among the participating agents. The purposeful force applied on the human must also be controlled in rehabilitation robotics applications, such as the one proposed by Krebs *et al.* (1998),[7] where the robot may directly affect patients' motion in order to help them track a desired trajectory. Since the contact force must be controlled with precision, a position-controlled could not be applied *a priori* in those circumstances, since small disturbances in the positioning could lead to large and dangerous interaction forces. However, in other applications, despite the constant need for a safe interaction, it is mainly the relative pose between robot and human that must be controlled. This is the case in the work of Soyama *et al.* (2004),[8] where a manipulator designed to feed subjects presenting upper limb impairments is described, and also in the work of Chen *et al.* (2013),[9] where a mobile manipulator is used to assist a physically impaired individual in tasks such as shaving.

In both applications where force or position control are required for effective pHRI, the corresponding tasks must be properly defined in order to be provided for the system controller to effectively control robots. Although simple verbal task definition is often enough for human understanding and cooperation, finding precise mathematical task descriptions for robot control may be a complex procedure. For this reason, despite the large number of works present in the literature exploring such interactions, usually they are focused on the execution of only specific tasks; for instance, cooperative carrying, handing over,[10] and crank-rotation.[11] It may be noted, however, that a large number of pHRIs may be described by the relative pose between the human hand and the robot hand. For instance, the task of pouring beverage into a cup can be completely defined by the geometric relation between the hands. Whenever handing over an object, the phase where the hands are moving toward each other can also be defined geometrically. For other tasks this description is not sufficient, since, for example, objects must be picked up before actual manipulation. However, even in this condition, the cooperative task itself may be described in terms of relative motions.

Considering the aforementioned taxonomy, in this paper we are mainly interested in pHRI tasks involving shared autonomy and where the task may be defined by the relative pose between human and robot, instead of being defined by the interaction force. Based on these specifications, the main goal of this work is to develop an appropriate kinematic model and a kinematic control strategy for pHRI that comprises different levels of shared autonomy.

1.1. Contributions and organization of the paper

We present a novel approach for kinematic modeling and control of pHRI systems that involve two-arm coordination and that use as basic description the relative configuration between the human hand and the robot hand. Since the relative configurations between human and robot are used to describe the interaction task, the control strategy results in robots performing reactive behaviors; i.e., the robot adapts its motion in reaction to the human's in order to obtain effective interaction. Furthermore, the method may also be applied for tasks requiring different interaction roles; for instance, interactions that incorporate complete or partial control of human arm, which might be particularly useful for applications involving physically impaired users.

In previous works, we presented preliminary development of kinematic modeling and control for pHRI,[12] as well as preliminary development regarding FES control of the human arm.[13] In the present paper, we unified the kinematic modeling and control of the interaction system from a more rigorous theoretical point of view. This development is important because we are able to show that complex interactions, when appropriately modeled, can be controlled using established control laws. Also, pHRIs that seem conceptual different can be generally modeled in the same way and controlled using the same control law. In addition, we also added comprehensive information on the low level control of the human arm using FES designed for the pHRI experiments described in this work. In particular, details on the closed-loop control of an antagonist muscle system and the initialization procedure that increases the overall FES stability are revealed.

The paper is organized as follows: the next section briefly presents the basic mathematical concepts used in the paper. Section 3 presents the kinematic modeling and control for pHRI, including a unified approach for two-arm coordination. Section 4 presents the low level control of the human arm by

means of FES, whereas Section 5 presents the experiments used to validate the proposed techniques. Last, Section 6 presents the discussion and conclusion, as well as some suggestions of future works. An appendix was also included in order to present some auxiliary mathematical proofs that were removed from the main text in order to improve readability.

2. Mathematical Background

A quaternion $\boldsymbol{h}$ consists of a real component plus an imaginary part composed of three quaternionic units $\hat{\imath}$, $\hat{\jmath}$, $\hat{k}$; that is,

$$\boldsymbol{h} = a + b\hat{\imath} + c\hat{\jmath} + d\hat{k},$$

where $a, b, c, d \in \mathbb{R}$, $\hat{\imath}^2 = \hat{\jmath}^2 = \hat{k}^2 = -1$ and $\hat{\imath}\hat{\jmath}\hat{k} = -1$. Its conjugate is given by $\boldsymbol{h^*} = a - b\hat{\imath} - c\hat{\jmath} - d\hat{k}$.

A rotation $\boldsymbol{r}$, composed of a rotation angle ϕ around the axis $\boldsymbol{n} = n_x\hat{\imath} + n_y\hat{\jmath} + n_z\hat{k}$, is given by the unit quaternion

$$\boldsymbol{r} = \cos(\phi/2) + \sin(\phi/2)\boldsymbol{n}.$$

A translation $\boldsymbol{p}$ is represented by a pure quaternion; that is, a quaternion where the real part is equal to zero. Thus,

$$\boldsymbol{p} = p_x\hat{\imath} + p_y\hat{\jmath} + p_z\hat{k}.$$

The dual quaternion

$$\underline{\boldsymbol{x}} = \boldsymbol{r} + \varepsilon\frac{1}{2}\boldsymbol{p}\boldsymbol{r} \tag{1}$$

represents a rigid motion composed of a translation quaternion $\boldsymbol{p}$ and a rotation quaternion $\boldsymbol{r}$, where ε is Clifford's dual unit.[14] The conjugate $\underline{\boldsymbol{x}}^*$ of the dual quaternion $\underline{\boldsymbol{x}}$ is given by

$$\underline{\boldsymbol{x}}^* = \boldsymbol{r}^* + \varepsilon\frac{1}{2}\boldsymbol{r}^*\boldsymbol{p}^*.$$

The term that is not multiplied by ε is usually called the primary part of the dual quaternion and the one multiplied by ε is called the dual part. Because both primary and dual parts are quaternions, (1) can be expanded such that a dual quaternion has the form

$$\underline{\boldsymbol{x}} = x_1 + x_2\hat{\imath} + x_3\hat{\jmath} + x_4\hat{k} + \varepsilon(x_5 + x_6\hat{\imath} + x_7\hat{\jmath} + x_8\hat{k}). \tag{2}$$

Definition 1. The vec operator performs the one-by-one mapping $\text{vec} : \mathcal{H} \to \mathbb{R}^8$; that is,

$$\text{vec}\,\underline{\boldsymbol{x}} = \begin{bmatrix} x_1 \\ \vdots \\ x_8 \end{bmatrix},$$

where $x_1 \ldots x_8$ are the coefficients of $\underline{\boldsymbol{x}}$ and $\mathcal{H}$ represents the set of dual quaternions.

Definition 2. Considering the dual quaternions $\underline{\boldsymbol{x}}_1$ and $\underline{\boldsymbol{x}}_2$, the Hamilton operators are the matrices $\overset{+}{\boldsymbol{H}}(\cdot)$ and $\overset{-}{\boldsymbol{H}}(\cdot)$ that satisfy[15,16]

$$\text{vec}(\underline{\boldsymbol{x}}_1\underline{\boldsymbol{x}}_2) = \overset{+}{\boldsymbol{H}}\left(\underline{\boldsymbol{x}}_1\right)\text{vec}\,\underline{\boldsymbol{x}}_2 = \overset{-}{\boldsymbol{H}}\left(\underline{\boldsymbol{x}}_2\right)\text{vec}\,\underline{\boldsymbol{x}}_1.$$

These two matrices in Definition 2 can be found by inspection. The great advantage of using them is that, although unit dual quaternions do not form a commutative group, Hamilton operators

https://doi.org/10.1017/S0263574714000356 Published online by Cambridge University Press

can be used to conveniently commute dual quaternions in complex expressions. This way, when the $\overset{+}{\boldsymbol{H}}(\cdot)$ operator is used the order of the operands in dual quaternion multiplication is maintained and, conversely, when the $\boldsymbol{H}(\cdot)$ operator is used the order of the operands in dual quaternion multiplication is inverted. The Hamilton operators will be particularly useful in the derivations of the kinematic models for pHRI in Section 3.

When used to represent the robot forward kinematic model (FKM), the dual quaternion $\underline{\boldsymbol{x}}$ is a function of the robot joint variables; that is,

$$\underline{\boldsymbol{x}} = \underline{\boldsymbol{f}}(\boldsymbol{\theta}),$$

where $\boldsymbol{\theta}$ is the n-dimensional vector of joint variables and $\underline{\boldsymbol{f}} : \mathbb{R}^n \to \mathcal{H}$. The differential FKM is given by

$$\operatorname{vec} \dot{\underline{\boldsymbol{x}}} = \boldsymbol{J}\dot{\boldsymbol{\theta}},$$

where $\boldsymbol{J}$ is the analytic Jacobian which can be found by using dual quaternion algebra.[16]

For a more complete treatment on the use of dual quaternions in robotics, please refer to the works of McCarthy (1990)[17] and Selig (2005).[14]

3. Kinematic Modeling and Control for pHRI

3.1. Kinematic modeling of the human-robot interaction system

In pHRI involving shared autonomy and defined by the relative configuration between human and robot, tasks are often executed within the two-arm coordination perspective; i.e., the coordination of movement between two end-effectors. For example, tasks such as handing over, pouring beverage into one's cup, and assisted shaving may be defined in this framework. In order to simplify the mathematical definition of such tasks, in this paper we have chosen to represent the two-arm coordination within the cooperative dual task-space framework,[18] which is based on dual quaternions to represent the relative configuration between the human hand and the robot hand. Other works also adopted the relative pose to describe cooperative tasks between manipulator robots,[19–24] but to the best of the authors' knowledge none of them extended or applied the cooperative manipulation formalism to the case of pHRI.

In order to represent the human-robot interaction in the cooperative dual task-space formalism, the arms of both robot and human are considered as manipulators sharing the same workspace and their end-effector configurations are represented by the dual quaternions $\underline{\boldsymbol{x}}_R^{\mathcal{T}}$ and $\underline{\boldsymbol{x}}_H^{\mathcal{T}}$, respectively, given with respect to a common frame $\mathcal{F}_{\mathcal{T}}$. The task, represented by the relative configuration between the arms, is given by

$$\begin{aligned} \underline{\boldsymbol{x}}_{\text{task}} &= \underline{\boldsymbol{x}}_R^{\mathcal{T}*}\underline{\boldsymbol{x}}_H^{\mathcal{T}} \\ &= \underline{\boldsymbol{x}}_H^R, \end{aligned} \tag{3}$$

where $\underline{\boldsymbol{x}}_R^{\mathcal{T}*}$ is the conjugate of $\underline{\boldsymbol{x}}_R^{\mathcal{T}}$. The advantage of describing the task by using (3) is that it does not depend on the common frame; that is, it depends only on the relationship between the human hand and the robot hand. Furthermore, (3) captures the kinematic constraints between the human hand and the robot hand. The dual quaternions corresponding to the relevant coordinate systems and the task are shown in Fig. 1.

Thus, given the task $\underline{\boldsymbol{x}}_{\text{task}}$, and the measured poses $\underline{\boldsymbol{x}}_{R_m}^{\mathcal{T}}$ and $\underline{\boldsymbol{x}}_{H_m}^{\mathcal{T}}$ of the robot hand and the human hand, respectively, the goal is to make $\underline{\boldsymbol{x}}_{R_m}^{\mathcal{T}*}\underline{\boldsymbol{x}}_{H_m}^{\mathcal{T}}$ converge to $\underline{\boldsymbol{x}}_{\text{task}}$. This can be accomplished by a kinematic control law that considers both human and robot as belonging to a single integrated system. In most cases, where humans behave autonomously, the terms corresponding to the control of human limbs can be simply zeroed out and the cooperative control law becomes equivalent to a standard kinematic control law, but which respects the geometric constraints imposed by the cooperative task. On the other hand, when impaired individuals (e.g., hemiplegics and quadriplegics) interact with robots, the interaction can be enhanced if the human limbs are artificially controlled, either

https://doi.org/10.1017/S0263574714000356 Published online by Cambridge University Press

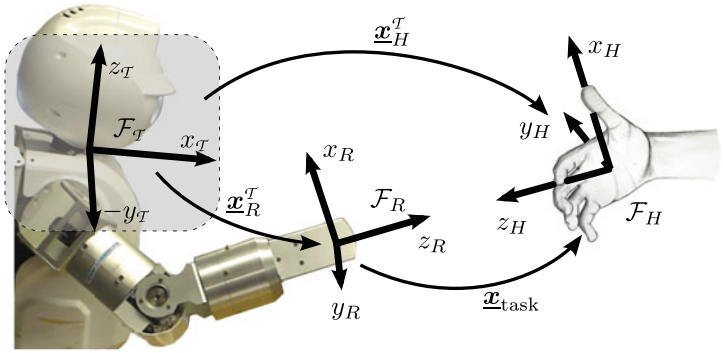

Fig. 1. Coordinate systems used in the cooperative dual task-space.

completely or partially. In these cases, it turns out, as will become evident later in this section, that kinematic control can be performed as well.

In order to develop appropriate kinematic controllers, let us proceed with the modeling of the differential kinematics of both human arm, robot arm, and human-robot interaction system.

The differential FKM of the robot arm is given by

$$\operatorname{vec} \dot{\underline{\boldsymbol{x}}}_R^{\mathcal{T}} = \boldsymbol{J}_{\underline{\boldsymbol{x}}_R^{\mathcal{T}}} \dot{\boldsymbol{\theta}}_R,$$

where $\boldsymbol{\theta}_R$ is the vector of joint variables of the robot arm, and $\boldsymbol{J}_{\underline{\boldsymbol{x}}_R^{\mathcal{T}}}$ is the analytic Jacobian of the robot arm, which can be found by using dual quaternion algebra.[16] Analogously, the differential FKM of the human arm is given by

$$\operatorname{vec} \dot{\underline{\boldsymbol{x}}}_H^{\mathcal{T}} = \boldsymbol{J}_{\underline{\boldsymbol{x}}_H^{\mathcal{T}}} \dot{\boldsymbol{\theta}}_H,$$

in which $\boldsymbol{\theta}_H$ is the vector of joint variables of the human arm, and $\boldsymbol{J}_{\underline{\boldsymbol{x}}_H^{\mathcal{T}}}$ is the analytic Jacobian of the human arm.[13]

Proposition 1. The unified differential FKM for the human-robot interaction system is given by

$$\operatorname{vec} \dot{\underline{\boldsymbol{x}}}_{\text{task}} = \boldsymbol{J}_{\text{task}} \dot{\boldsymbol{\theta}}_C, \tag{4}$$

where $\underline{\boldsymbol{x}}_{\text{task}}$ is given by (3), $\boldsymbol{\theta}_C$ is the vector of joint variables of the cooperative system; that is,

$$\boldsymbol{\theta}_C \triangleq \begin{bmatrix} \boldsymbol{\theta}_R \\ \boldsymbol{\theta}_H \end{bmatrix}, \tag{5}$$

and the task Jacobian $\boldsymbol{J}_{\text{task}}$ is given by

$$\boldsymbol{J}_{\text{task}} = \begin{bmatrix} \bar{\boldsymbol{H}}\left(\underline{\boldsymbol{x}}_H^{\mathcal{T}}\right) \boldsymbol{C}_8 \boldsymbol{J}_{\underline{\boldsymbol{x}}_R^{\mathcal{T}}} & \overset{+}{\boldsymbol{H}}\left(\underline{\boldsymbol{x}}_R^{\mathcal{T}*}\right) \boldsymbol{J}_{\underline{\boldsymbol{x}}_H^{\mathcal{T}}} \end{bmatrix}, \tag{6}$$

where

$$\boldsymbol{C}_8 = \operatorname{diag}(1, -1, -1, -1, 1, -1, -1 - 1). \tag{7}$$

Proof. Taking the first derivative of (3), one obtains

$$\dot{\underline{\boldsymbol{x}}}_{\text{task}} = \dot{\underline{\boldsymbol{x}}}_R^{\mathcal{T}*} \underline{\boldsymbol{x}}_H^{\mathcal{T}} + \underline{\boldsymbol{x}}_R^{\mathcal{T}*} \dot{\underline{\boldsymbol{x}}}_H^{\mathcal{T}}$$

$$\operatorname{vec} \dot{\underline{\boldsymbol{x}}}_{\text{task}} = \bar{\boldsymbol{H}}\left(\underline{\boldsymbol{x}}_H^{\mathcal{T}}\right) \operatorname{vec} \dot{\underline{\boldsymbol{x}}}_R^{\mathcal{T}*} + \overset{+}{\boldsymbol{H}}\left(\underline{\boldsymbol{x}}_R^{\mathcal{T}*}\right) \operatorname{vec} \dot{\underline{\boldsymbol{x}}}_H^{\mathcal{T}}.$$

https://doi.org/10.1017/S0263574714000356 Published online by Cambridge University Press

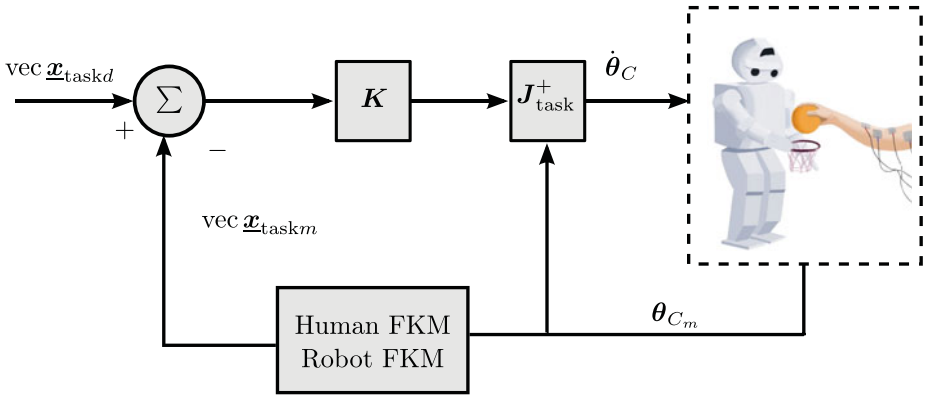

Fig. 2. Block diagram corresponding to the cooperative control law given by (8). The controller provides joint velocity vectors for the human arm and the robot arm, which are considered as subsystems of the unified system.

Since $\text{vec}\,\underline{\dot{\boldsymbol{x}}}_R^{\mathcal{T}} = \boldsymbol{J}_{\underline{\boldsymbol{x}}_H^{\mathcal{T}}}\dot{\boldsymbol{\theta}}_R$, hence $\text{vec}\,\underline{\dot{\boldsymbol{x}}}_R^{\mathcal{T}*} = \boldsymbol{C}_8\boldsymbol{J}_{\underline{\boldsymbol{x}}_R^{\mathcal{T}}}\dot{\boldsymbol{\theta}}_R$. Thus,

$$\begin{aligned}\text{vec}\,\underline{\dot{\boldsymbol{x}}}_{\text{task}} &= \bar{\boldsymbol{H}}\left(\underline{\boldsymbol{x}}_H^{\mathcal{T}}\right)\boldsymbol{C}_8\boldsymbol{J}_{\underline{\boldsymbol{x}}_R^{\mathcal{T}}}\dot{\boldsymbol{\theta}}_R + \overset{+}{\boldsymbol{H}}\left(\underline{\boldsymbol{x}}_R^{\mathcal{T}*}\right)\boldsymbol{J}_{\underline{\boldsymbol{x}}_H^{\mathcal{T}}}\dot{\boldsymbol{\theta}}_H \\ &= \left[\bar{\boldsymbol{H}}\left(\underline{\boldsymbol{x}}_H^{\mathcal{T}}\right)\boldsymbol{C}_8\boldsymbol{J}_{\underline{\boldsymbol{x}}_R^{\mathcal{T}}} \quad \overset{+}{\boldsymbol{H}}\left(\underline{\boldsymbol{x}}_R^{\mathcal{T}*}\right)\boldsymbol{J}_{\underline{\boldsymbol{x}}_H^{\mathcal{T}}}\right]\dot{\boldsymbol{\theta}}_C \\ &= \boldsymbol{J}_{\text{task}}\dot{\boldsymbol{\theta}}_C.\end{aligned}$$

□

It is important to note that both $\boldsymbol{J}_{\underline{\boldsymbol{x}}_R^{\mathcal{T}}}$ and $\boldsymbol{J}_{\underline{\boldsymbol{x}}_H^{\mathcal{T}}}$ are expressed with respect to the common base frame $\mathcal{F}_{\mathcal{T}}$. The task Jacobian $\boldsymbol{J}_{\text{task}}$, however, is expressed with respect to the task frame $\mathcal{F}_R$.

3.2. Kinematic control of the interaction system

In order to close the loop at the interaction level and considering both human and robot as a unified interaction system, one can apply the stable control law based on dual quaternions:[18,25]

$$\dot{\boldsymbol{\theta}}_C = \boldsymbol{J}^{+}_{\text{task}}\boldsymbol{K}\,\text{vec}(\underline{\boldsymbol{x}}_{\text{task}\,d} - \underline{\boldsymbol{x}}_{\text{task}\,m}), \tag{8}$$

where $\underline{\boldsymbol{x}}_{\text{task}\,d}$ and $\underline{\boldsymbol{x}}_{\text{task}\,m}$ are the desired and measured values of the dual quaternions corresponding to the task, $\boldsymbol{K} \in \mathbb{R}^{8\times 8}$ is a positive definite gain matrix, and $\boldsymbol{J}^{+}_{\text{task}}$ is the pseudoinverse of the task Jacobian, which is calculated using the measured joint variables. Alternatively, instead of using the pseudoinverse of the task Jacobian, one can use techniques that are robust to singularities (e.g., damped least-squares inverse, damped least-squares inverse with numerical filtering, etc.[26]) Also, the gain matrix can be chosen according to a H_∞ robust control criterion.[27] The block diagram corresponding to (8) is shown in Fig. 2.

Once the joint velocity $\dot{\boldsymbol{\theta}}_C$ of the cooperative system is calculated by using (8), it is provided for inner low level controllers that are responsible to perform the joint position control of the robot arm and the joint velocity control of the human arm (Fig. 3).

It is important to highlight that the control law (8) can be considered as belonging to the class of the closed-loop inverse kinematics algorithms (CLIK).[28] However, thanks to the suitable model derived in the previous section, this control law takes into account the kinematic constraints of the interaction task; that is, the loop is closed at the interaction level.

3.2.1. Different interaction roles. The cooperative control law (8) can also be used to control tasks involving different interaction roles between robot and human. Within the most usual applications, the robot motion is controlled based on the measured human movement. However, it may be the case that the human hand is completely or partially controlled to maximize success in performing

https://doi.org/10.1017/S0263574714000356 Published online by Cambridge University Press

the task. Human movement control may be performed using different technologies, such as active exoskeletons and FES (see Section 4). This application might be particularly useful for individuals presenting severe physical impairments.

In order to implement such functionalities, the correspondent joint velocities are simply zeroed out; for instance, if the human arm is not controlled or moves autonomously, $\dot{\boldsymbol{\theta}}_H \leftarrow \mathbf{0}$, whereas if the robot arm is not controlled, $\dot{\boldsymbol{\theta}}_R \leftarrow \mathbf{0}$. However, in those particular cases it can be more convenient to use equivalent control laws, as shown in Propositions 2 and 3.

Proposition 2. When the human arm is not controlled, the control law (8) is equivalent to

$$\dot{\boldsymbol{\theta}}_R = \boldsymbol{J}^{+}_{\underline{\boldsymbol{x}}^{\mathcal{T}}_R} \boldsymbol{K}_1 \operatorname{vec}\left(\underline{\boldsymbol{x}}^{\mathcal{T}}_{R_d} - \underline{\boldsymbol{x}}^{\mathcal{T}}_{R_m}\right), \tag{9}$$

where

$$\boldsymbol{K}_1 = \boldsymbol{C}_8 \bar{\boldsymbol{H}}\left(\underline{\boldsymbol{x}}^{\mathcal{T}*}_{H_m}\right) \boldsymbol{K} \bar{\boldsymbol{H}}\left(\underline{\boldsymbol{x}}^{\mathcal{T}}_{H_m}\right) \boldsymbol{C}_8,$$

$\underline{\boldsymbol{x}}^{\mathcal{T}}_{R_d} = \underline{\boldsymbol{x}}^{\mathcal{T}}_{H_m} \underline{\boldsymbol{x}}^{*}_{\text{task}\,d}$, and $\underline{\boldsymbol{x}}^{\mathcal{T}}_{H_m}$ and $\underline{\boldsymbol{x}}^{\mathcal{T}}_{R_m}$ are the current poses of the human hand and the robot hand, respectively, measured with respect to a common frame $\mathcal{F}_{\mathcal{T}}$.

Proof. When the human arm is not controlled, deviations from the desired value of the task parameters have no effect in the value of the joint variables of the human arm. In terms of the control law (8), this is equivalent to say that $\dot{\boldsymbol{\theta}}_H = \mathbf{0}$; thus,

$$\boldsymbol{J}_{\text{task}} = \bar{\boldsymbol{H}}\left(\underline{\boldsymbol{x}}^{\mathcal{T}}_{H_m}\right) \boldsymbol{C}_8 \boldsymbol{J}_{\underline{\boldsymbol{x}}^{\mathcal{T}}_R},$$

with $\boldsymbol{C}_8$ defined in (7).

The control law (8) becomes

$$\dot{\boldsymbol{\theta}}_R = \boldsymbol{J}^{+}_{\underline{\boldsymbol{x}}^{\mathcal{T}}_R} \boldsymbol{C}_8^{+} \bar{\boldsymbol{H}}\left(\underline{\boldsymbol{x}}^{\mathcal{T}}_{H_m}\right)^{+} \boldsymbol{K} \operatorname{vec}\left(\underline{\boldsymbol{x}}_{\text{task}\,d} - \underline{\boldsymbol{x}}^{\mathcal{T}*}_{R_m} \underline{\boldsymbol{x}}^{\mathcal{T}}_{H_m}\right).$$

Since $\bar{\boldsymbol{H}}\left(\underline{\boldsymbol{x}}^{\mathcal{T}}_{H_m}\right)^{+} = \bar{\boldsymbol{H}}\left(\underline{\boldsymbol{x}}^{\mathcal{T}*}_{H_m}\right)$ (see Fact 1 in Appendix A), $\boldsymbol{C}_8^{+} = \boldsymbol{C}_8$, and

$$\begin{aligned}\boldsymbol{C}_8^{+} \bar{\boldsymbol{H}}\left(\underline{\boldsymbol{x}}^{\mathcal{T}}_{H_m}\right)^{+} \boldsymbol{K} &= \boldsymbol{C}_8 \bar{\boldsymbol{H}}\left(\underline{\boldsymbol{x}}^{\mathcal{T}*}_{H_m}\right) \boldsymbol{K} \bar{\boldsymbol{H}}\left(\underline{\boldsymbol{x}}^{\mathcal{T}}_{H_m}\right) \boldsymbol{C}_8 \boldsymbol{C}_8 \bar{\boldsymbol{H}}\left(\underline{\boldsymbol{x}}^{\mathcal{T}*}_{H_m}\right) \\ &= \boldsymbol{K}_1 \boldsymbol{C}_8 \bar{\boldsymbol{H}}\left(\underline{\boldsymbol{x}}^{\mathcal{T}*}_{H_m}\right),\end{aligned}$$

then

$$\begin{aligned}\dot{\boldsymbol{\theta}}_R &= \boldsymbol{J}^{+}_{\underline{\boldsymbol{x}}^{\mathcal{T}}_R} \boldsymbol{C}_8 \bar{\boldsymbol{H}}\left(\underline{\boldsymbol{x}}^{\mathcal{T}*}_{H_m}\right) \boldsymbol{K} \operatorname{vec}\left(\underline{\boldsymbol{x}}_{\text{task}\,d} - \underline{\boldsymbol{x}}^{\mathcal{T}*}_{R_m} \underline{\boldsymbol{x}}^{\mathcal{T}}_{H_m}\right) \\ &= \boldsymbol{J}^{+}_{\underline{\boldsymbol{x}}^{\mathcal{T}}_R} \boldsymbol{K}_1 \boldsymbol{C}_8 \bar{\boldsymbol{H}}\left(\underline{\boldsymbol{x}}^{\mathcal{T}*}_{H_m}\right) \operatorname{vec}\left(\underline{\boldsymbol{x}}_{\text{task}\,d} - \underline{\boldsymbol{x}}^{\mathcal{T}*}_{R_m} \underline{\boldsymbol{x}}^{\mathcal{T}}_{H_m}\right) \\ &= \boldsymbol{J}^{+}_{\underline{\boldsymbol{x}}^{\mathcal{T}}_R} \boldsymbol{K}_1 \boldsymbol{C}_8 \operatorname{vec}\left(\underline{\boldsymbol{x}}_{\text{task}\,d} \underline{\boldsymbol{x}}^{\mathcal{T}*}_{H_m} - \underline{\boldsymbol{x}}^{\mathcal{T}*}_{R_m}\right) \\ &= \boldsymbol{J}^{+}_{\underline{\boldsymbol{x}}^{\mathcal{T}}_R} \boldsymbol{K}_1 \operatorname{vec}\left(\underline{\boldsymbol{x}}^{\mathcal{T}}_{H_m} \underline{\boldsymbol{x}}^{*}_{\text{task}\,d} - \underline{\boldsymbol{x}}^{\mathcal{T}}_{R_m}\right).\end{aligned}$$

It is important to note that, if $\boldsymbol{K}$ is positive definite, then $\boldsymbol{K}_1$ is also positive definite (see Fact 3 in Appendix A). □

Proposition 3. When the robot arm is not actuated, the control law (8) is equivalent to

$$\dot{\boldsymbol{\theta}}_H = \boldsymbol{J}^{+}_{\underline{\boldsymbol{x}}^{\mathcal{T}}_H} \boldsymbol{K}_1 \operatorname{vec}\left(\underline{\boldsymbol{x}}^{\mathcal{T}}_{H_d} - \underline{\boldsymbol{x}}^{\mathcal{T}}_{H_m}\right), \tag{10}$$

https://doi.org/10.1017/S0263574714000356 Published online by Cambridge University Press

where $\underline{\boldsymbol{x}}_{H_d}^{\mathcal{T}} = \underline{\boldsymbol{x}}_{R_m}^{\mathcal{T}} \underline{\boldsymbol{x}}_{\text{task}\,d}$ and

$$\boldsymbol{K}_1 = \overset{+}{\boldsymbol{H}} \left(\underline{\boldsymbol{x}}_{R_m}^{\mathcal{T}}\right) \boldsymbol{K} \overset{+}{\boldsymbol{H}} \left(\underline{\boldsymbol{x}}_{R_m}^{\mathcal{T}*}\right).$$

Proof. The reasoning is analogous to the one of Proposition 2; that is, in terms of the control law (8), $\dot{\boldsymbol{\theta}}_R = \boldsymbol{0}$. In this way, $\boldsymbol{J}_{\text{task}} = \overset{+}{\boldsymbol{H}} \left(\underline{\boldsymbol{x}}_R^{\mathcal{T}*}\right) \boldsymbol{J}_{\underline{\boldsymbol{x}}_H^{\mathcal{T}}}$ and the control law (8) becomes

$$\dot{\boldsymbol{\theta}}_H = \boldsymbol{J}_{\underline{\boldsymbol{x}}_H^{\mathcal{T}}}^{+} \overset{+}{\boldsymbol{H}} \left(\underline{\boldsymbol{x}}_{R_m}^{\mathcal{T}*}\right)^{+} \boldsymbol{K}\, \text{vec}\left(\underline{\boldsymbol{x}}_{\text{task}\,d} - \underline{\boldsymbol{x}}_{R_m}^{\mathcal{T}*} \underline{\boldsymbol{x}}_{H_m}^{\mathcal{T}}\right).$$

Since $\overset{+}{\boldsymbol{H}} \left(\underline{\boldsymbol{x}}_{R_m}^{\mathcal{T}*}\right)^{+} = \overset{+}{\boldsymbol{H}} \left(\underline{\boldsymbol{x}}_{R_m}^{\mathcal{T}}\right)$ (see Fact 2 in Appendix A), then

$$\begin{aligned}
\dot{\boldsymbol{\theta}}_H &= \boldsymbol{J}_{\underline{\boldsymbol{x}}_H^{\mathcal{T}}}^{+} \overset{+}{\boldsymbol{H}} \left(\underline{\boldsymbol{x}}_{R_m}^{\mathcal{T}}\right) \boldsymbol{K}\, \text{vec}\left(\underline{\boldsymbol{x}}_{\text{task}\,d} - \underline{\boldsymbol{x}}_{R_m}^{\mathcal{T}*} \underline{\boldsymbol{x}}_{H_m}^{\mathcal{T}}\right) \\
&= \boldsymbol{J}_{\underline{\boldsymbol{x}}_H^{\mathcal{T}}}^{+} \overset{+}{\boldsymbol{H}} \left(\underline{\boldsymbol{x}}_{R_m}^{\mathcal{T}}\right) \boldsymbol{K} \overset{+}{\boldsymbol{H}} \left(\underline{\boldsymbol{x}}_{R_m}^{\mathcal{T}*}\right) \overset{+}{\boldsymbol{H}} \left(\underline{\boldsymbol{x}}_{R_m}^{\mathcal{T}}\right) \text{vec}\left(\underline{\boldsymbol{x}}_{\text{task}\,d} - \underline{\boldsymbol{x}}_{R_m}^{\mathcal{T}*} \underline{\boldsymbol{x}}_{H_m}^{\mathcal{T}}\right) \\
&= \boldsymbol{J}_{\underline{\boldsymbol{x}}_H^{\mathcal{T}}}^{+} \boldsymbol{K}_1 \overset{+}{\boldsymbol{H}} \left(\underline{\boldsymbol{x}}_{R_m}^{\mathcal{T}}\right) \text{vec}\left(\underline{\boldsymbol{x}}_{\text{task}\,d} - \underline{\boldsymbol{x}}_{R_m}^{\mathcal{T}*} \underline{\boldsymbol{x}}_{H_m}^{\mathcal{T}}\right) \\
&= \boldsymbol{J}_{\underline{\boldsymbol{x}}_H^{\mathcal{T}}}^{+} \boldsymbol{K}_1 \text{vec}\left(\underline{\boldsymbol{x}}_{R_m}^{\mathcal{T}} \underline{\boldsymbol{x}}_{\text{task}\,d} - \underline{\boldsymbol{x}}_{H_m}^{\mathcal{T}}\right).
\end{aligned}$$

It is important to note that, if $\boldsymbol{K}$ is positive definite, then $\boldsymbol{K}_1$ is also positive definite (the argument of proof is similar to the one of Fact 3 in Appendix A). □

The cooperative control law (8) can consequently be used when both agents are controlled, or when only one agent is controlled. It is important to underline that, in any case, the control law is closed loop at the interaction level, since it takes into consideration the geometric constraint of the task.

From Fig. 2, one may observe that the joint positions are controlled by inner low level controllers. If on the one hand most commercial robots possess built-in PD controllers for each joint—which is the case for the robot used in our work—on the other hand it is not obvious to access the low level controllers of the human arm. In this case, one must bypass the natural motor control mechanisms, which imposes two challenges: first, the human arm must somehow be artificially actuated and, second, it must be controlled at the low level. These issues are addressed in the next section.

4. Low Level Control of the Human Arm Using FES

Different technologies, such as active orthoses and FES are available to affect or directly induce motion of human limbs. In this work we have opted to use FES, which is based on the principle of delivering electric pulses to the muscle motor point, inducing muscle action and consequently joint motion.[29] Among the advantages of employing FES in pHRI experiments, the use of the human's own muscles as actuators and the concomitant stimulation of afferent pathways motivates the choice of FES with respect to alternative technologies. Both features may provide important benefits in a physical rehabilitation scenario, which is a prospective application of this work.

Typically, FES control systems either apply open-loop or closed-loop control schemes to induce a target motion. Due to the model complexity and practical issues related to the use of surface stimulation, in this work, instead of applying model-based control strategies, we have used a PI controller with anti-windup,[30] as illustrated in Fig 3. The need of anti-windup is due to actuator saturation imposed by physiological limits and to provide comfort to the subjects.

A single normalized control variable u, with $-1 \leq u \leq 1$, is defined to incorporate the stimulation levels of both stimulated antagonist muscles. Hence, a strategy must be defined in order to compute the individual activation levels for each muscle that compose the antagonist system. In this work, we assume that no co-activation occurs between antagonist muscles, and also that the muscles provide identical maximum torque to the joint. Although this is a simplified assumption when compared to

https://doi.org/10.1017/S0263574714000356 Published online by Cambridge University Press

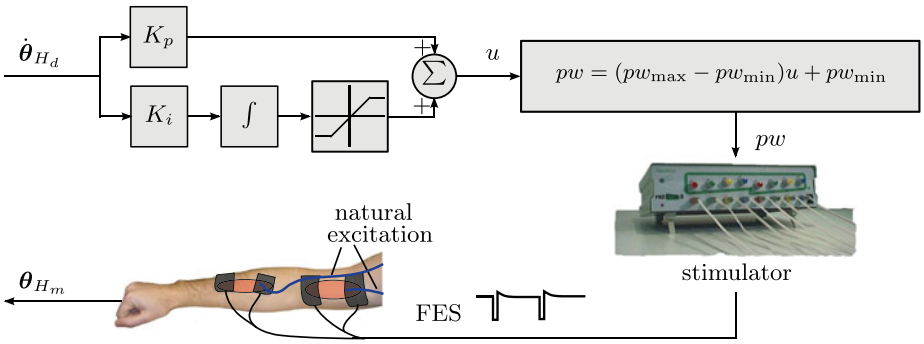

Fig. 3. Low level control of the human arm using FES.

human motor control, it has enabled straightforward computation of the individual stimulation levels u_f (flexor muscle) and u_e (extensor muscle):

$$u_f = \begin{cases} u, & u > 0 \\ 0, & u \leq 0 \end{cases} \quad \text{and} \quad u_e = \begin{cases} \|u\|, & u < 0 \\ 0, & u \geq 0 \end{cases}.$$

Based on these individual control variables which define the stimulation intensity for each muscle, FES parameters may then be updated in order to change the muscle activation level. Normally, FES signals are composed of trains of electric pulses, while the modulation of the charge delivered to the muscle enables control of the number of recruited muscle fibers. Within this work, the control of delivered charge is performed using pulse-width modulation. In this way, if the static stimulation frequency and amplitude are high enough, smooth and sustained contractions of different levels can be generated. One important advantage of FES systems for pHRI experiments is that, in order to adjust the setup for new users, only one parameter must be updated for each stimulated muscle: the amplitude, in [mA], of the electric pulses. This parameter was chosen during an initialization procedure, in which FES amplitudes that would provide similar motor response for antagonist muscles were selected. The overall procedure used to control the elbow joint is summarized in Fig. 3.

For opening the hand, precise control was not needed. For that reason, FES was used in an on/off control scheme, where the hand switches between two states: relaxed or fully opened.

Figure 4 shows the performance of the FES system in controlling the elbow joint. The data refers to different trials belonging to the experiment described in Section 5.3, where the reference for the human arm motion was determined dynamically using (8). Since similar reference signals are generated, the corresponding patterns of u were equally similar. Due to these comparable applied stimulation intensities, the figure also serves to illustrate the high level of repeatability achieved by the low level control of the human arm.

5. Experiments[1]

In order to validate the proposed method, we performed experiments in the context of three different tasks. They were designed to encompass all aspects related to the definition of pHRI using relative configurations, and also the ones related to the reactive behavior of the robot during task execution, and the different interaction roles that robot and human may assume within the considered scenario. The first experiment, called *mirrored movements followed by simultaneous handling*, was used to evaluate the situation in which the human assumes the role of master and the robot plays the role of slave; in the second experiment—called *ball in the hoop*—the roles were inverted such that the robot held complete control of the task, as it controlled the human arm by means of FES. Lastly, the *pouring water* experiment was designed to assess the situation where only the robot arm is controlled and, from the point of view of an external observer, both agents are regarded as autonomous entities.

[1] See provided video #1 with the recorded experiments.

https://doi.org/10.1017/S0263574714000356 Published online by Cambridge University Press

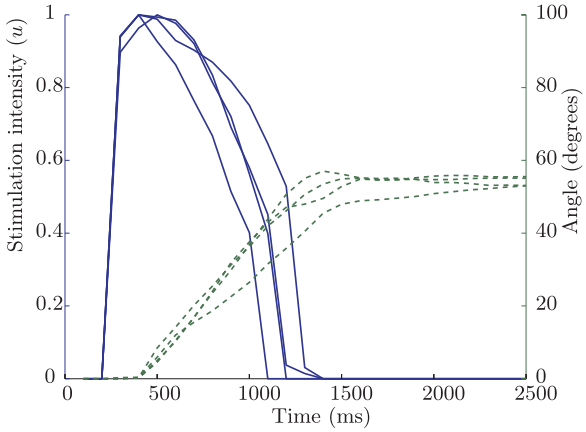

Fig. 4. Different trials from the same subject, wherein closed-loop control of the human elbow joint position (*dashed*) was performed using FES, and the performance of the controller in terms of repeatability may be observed. The corresponding normalized FES control signals (*solid*) are also shown to illustrate the system dynamics. The FES signals applied into muscles are characterized by trains of electric pulses, with fixed frequency (40 Hz) and fixed amplitude (∼10 mA). The intensity of stimulation is updated using pulse-width modulation, where the maximum value of the normalized control signal is 1 and corresponds to 150 μs.

5.1. General experimental setup

The robot used in all experiments was a Hoap-3 (Fujitsu, Japan) humanoid robot, which is 60 cm tall, weighs about 8 kg, and has 28 DOFs, with each arm having four DOFs. The kinematic controller (8) used for the interaction system was run on Matlab using a non realtime system with a sample time of approximately 100 ms. A diagonal gain matrix $\boldsymbol{K} \in \mathbb{R}^{8\times 8}$, with the first four diagonal elements equal to 0.003 and the last four diagonal elements equal to 0.03, was chosen empirically in order to have smooth behavior and satisfactory performance in terms of time response. The robot runs a legacy realtime operating system (RT-Linux) on an embedded PC card Intel Pentium M Processor 1.1 GHz. There is a DC motor in each joint axis with an embedded microcontroller linked with the PC card by using realtime USB connexion, which was developed by Fujitsu Lab. In each microcontroller there is a dedicated PD controller running at 1 kHz, also developed by Fujitsu Lab. In this work, we used the joint PD-controllers with the default gain values provided by the robot manufacturer.

Only healthy subjects participated in the experiments, and both the robot and the person used the right arm for the cooperative tasks, as shown in Fig. 5, which also illustrates the main coordinate systems used in the experiments. Since the task is defined by the relative configuration between the hands, their poses must be estimated. The pose of the robot end-effector is given by the FKM whereas the human hand pose was measured using an optical motion tracker.

The problem of this setup is that the robot hand is related to $\mathcal{F}_T$, whereas the pose of the human hand is related to $\mathcal{F}_M$, the coordinate system of the motion tracker. However, (3) requires that the poses of both the human hand and the robot hand be expressed with respect to a common frame, which was chosen as the robot torso. For the purposes of this paper, all the reasoning is done by assuming that the pose of the human hand is already given with respect to the common frame, and the methodology to obtain such pose is presented in previous works.[12,13]

The motion tracker used in this work, the Easytrack 500 (Atracsys, Switzerland), is composed of linear cameras and can track and estimate, every 100 ms, the pose of a marker equipped with infrared LEDs. In the first two experiments, the marker was placed on the subject's wrist or hand, as shown in Figs. 6 and 10, defining the frame $\mathcal{F}_H$, whereas in the last experiment (*ball in the hoop*) the marker was placed on the ball.

For the *ball in the hoop* experiment, an 8-channel stimulator—called Prostim (DEMAR/ Neuromedics, France)—was used to artificially control human motion.

5.2. Human holds complete control: mirrored movements followed by simultaneous handling

As the name suggests, mirrored movements are characterized by motions analogous to the ones that one can see in front of a mirror. Considering a pHRI task, while the human master performs a motion,

https://doi.org/10.1017/S0263574714000356 Published online by Cambridge University Press

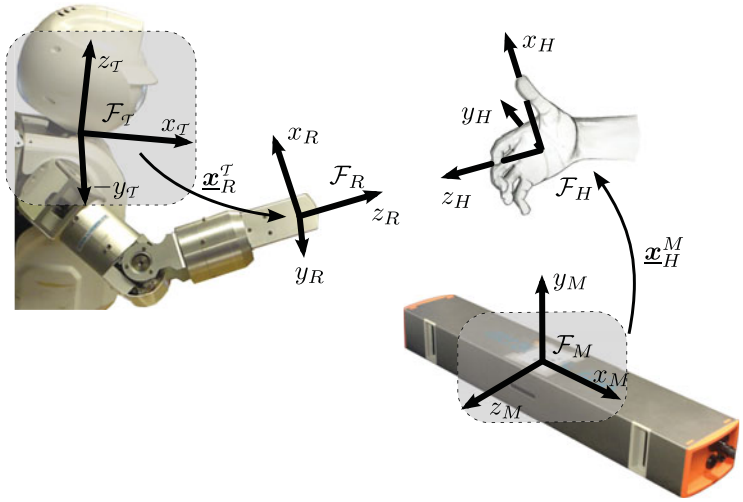

Fig. 5. Experimental setup for the human-robot interaction.

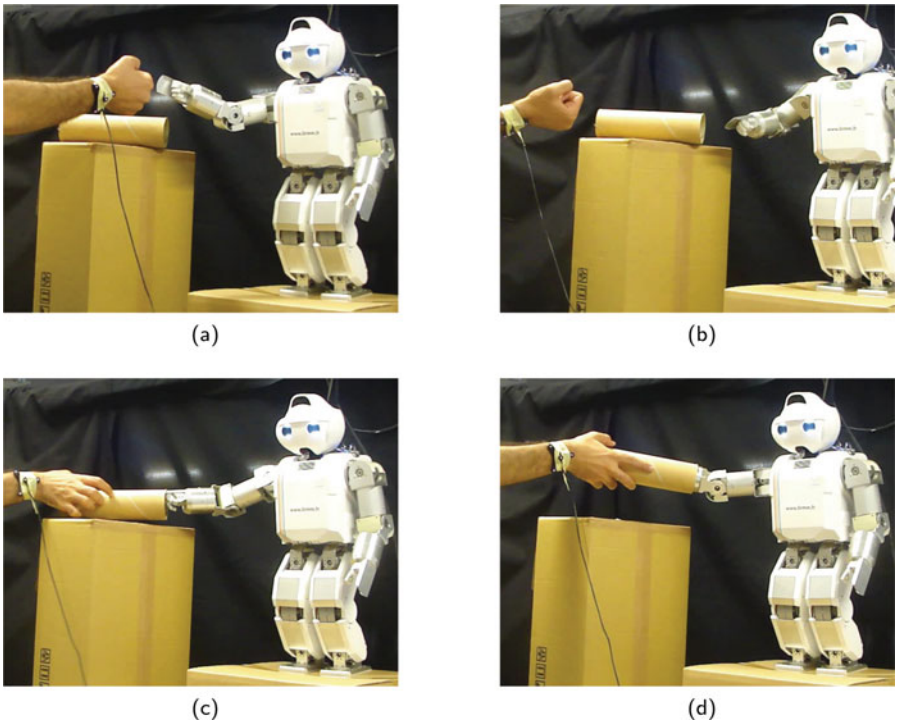

Fig. 6. Mirror mode: the person controls the robot in a collaboration-like fashion. (*a*) The system is initialized in the face-to-face configuration; (*b*) the subject's hand is moved backward. The robot mirrors the movement; (*c*) the subject drives his hand toward the object, and the robot symmetrically follows the movement; (*d*) once the object is grasped, the current $\underline{\boldsymbol{x}}_{\text{task}\,m}$ is stored and remains constant; that is, $\underline{\boldsymbol{x}}_{\text{task}\,d} \leftarrow \underline{\boldsymbol{x}}_{\text{task}\,m}$. Since the subject's arm has more DOFs than the robot's, the subject can still move the object, followed by the robot. Please refer to provided video #1 for the complete execution of this experiment.

the reactive robot will play the role of a mirror. In one potential application, the person may use the mirrored movements to drive the robot hand to grasp an object of interest.

In order to illustrate this idea, we have designed the following experiment. The person must grab an object but needs help to accomplish the task, because the object is too heavy or too big, for example. This task was already extensively investigated in terms of force control (e.g., Stasse *et al.* (2009)[31]), where the robot follows the person by means of force compliance. However, before the activation of

https://doi.org/10.1017/S0263574714000356 Published online by Cambridge University Press

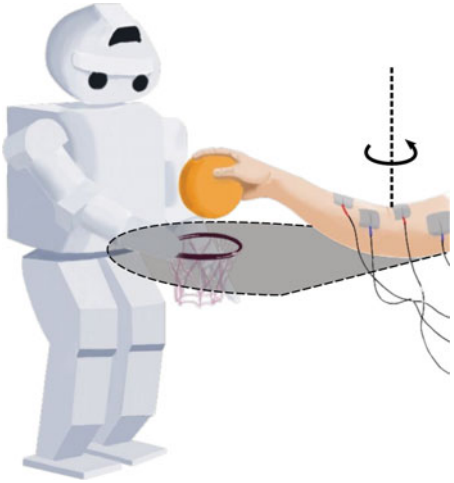

Fig. 7. In the ball in the hoop experiment, the human arm was actuated by FES and was constrained to move in a plane.

the force controllers, the robot should reach the object. If the robot mirrors the person, the person can drive the robot hand to the right grasp position while positioning his own hand.

By using the variable task parameter $\underline{\boldsymbol{x}}_{\text{task}\,d}$ defined in Adorno *et al.* (2011),[13] the robot behaves as follows: whenever the subject moves his hand vertically or horizontally, the robot will try to place its hand at the same place as the subject's hand. However, when the subject moves the hand backward, the robot will also move its hand backward. Conversely, when the subject moves the hand forward, the robot will move its hand forward.

Figure 6(a)–(c) show the sequence obtained from a manipulation task using mirrored movements. First, the system was initialized in the face-to-face configuration. Then, the operator directed his hand toward one extremity of the pipe while simultaneously controlling the robot's hand. Differently from a simple teleoperation, in this type of task the operator must take into account the poses of both his hand and the robot's in order to simultaneously grasp the pipe.

After the pipe was handled, the current value of $\underline{\boldsymbol{x}}_{\text{task}\,m}$ was stored and from that moment the stored value was used as a constant reference; that is, $\underline{\boldsymbol{x}}_{\text{task}\,d} \leftarrow \underline{\boldsymbol{x}}_{\text{task}\,m}$. In this new subtask the robot had to maintain the same relative configuration. The remarkable finding is that, even if the object was rigid and the robot was position controlled—and thus very stiff—the operator could still drive the pipe and was followed by the robot. This was thanks to the fact that the human arm has more DOFs than the robot's, and hence the operator could exploit this redundancy to maintain the pipe in the same orientation of his hand, but changing the orientation of his wrist. Consequently, the robot followed the operator's movement. Moreover, the forces involved in such interaction are measured by the person's force feedback mechanism, and even if the robot was not capable of performing force control, the human was. Hence, in simultaneous handling tasks, the *human* ultimately takes into account the forces involved in the interaction, and consequently can adjust the pose of his arm in order to minimize these interaction forces.

5.3. Robot holds complete control: the ball in the hoop *task*

The *ball in the hoop* task was defined such that the robot had to hold a miniature basketball hoop and the person had to hold a ball. The human arm was controlled by means of FES and both robot arm and human arm had to be coordinated in order to drop the ball inside the hoop. To simplify the experimental setup and avoid the requirements of precise multi-joint FES control, the human arm was constrained to move only in one plane, as depicted in Fig. 7. In this way, controlling just the elbow was enough to accomplish the task. In order to control the elbow, only the *Biceps Brachii* was stimulated, which means that the FES system was not able to extend the elbow (i.e., $u_e = 0$). Opening the hand was achieved by activating the *Extensor Digitorum Communis*. To use the control law (8)—and considering the restrictions of our current implementation of the FES controller—we modeled the human arm as a one-DOF serial robot with the rotation axis located at the elbow and the

https://doi.org/10.1017/S0263574714000356 Published online by Cambridge University Press

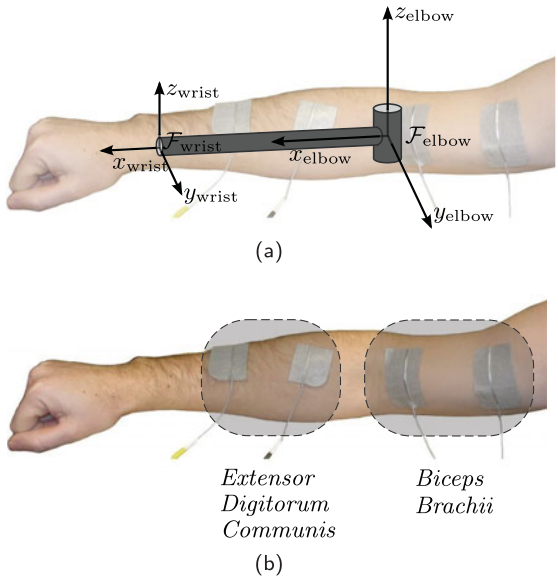

Fig. 8. The human arm modeled as a one-link serial robot (*top*) and positioning of the electrodes for the actuation of the human arm (*bottom*).

end-effector located at the wrist, as illustrated in Fig. 8(a). The placement of the electrodes is shown in Fig. 8(b).

Five healthy volunteers participated in the experiment, three males and two females. They were positioned with the arms standing over a surface parallel to the robot's floor. Furthermore, the subjects were blindfolded in order to prevent visual feedback and thus to prevent any attempt to accomplish the task by natural actuation; that is, not by means of the FES. In addition, they were asked to not move their bodies and to avoid the voluntary control of their arms—although they could not completely control their biceps, in principle they could disturb the task by controlling other muscles involved in the movement of the arm.

The task was divided into "reaching" and "dropping the ball" subtasks. First, the "reaching" subtask had to be performed by aligning the hands along a vertical line, under the assumption that the human hand was higher than the robot hand. For this, first $\dot{\boldsymbol{\theta}}_R$ was zeroed out, such that (8) became equivalent to (10) and only the human arm was controlled in order to bring it into the robot's workspace—typically in a predefined region known to be suitable to accomplish the cooperative task—e.g., the center of the robot's workspace. The value of $\dot{\boldsymbol{\theta}}_H$ was then provided for the low level FES controller to control the human elbow joint. Once the human hand was inside the robot's workspace, the control law (8) was used with no terms zeroed out—that is, providing full coordination—until the moment that the hands would be aligned. From that moment, both robot arm and human biceps were not controlled anymore, and then the robot sent the FES signal to open the human hand and drop the ball inside the hoop.

Figure 9 shows a successful cooperation sequence: the human arm entered the cooperation zone in about one second, but the "dropping the ball" subtask could not be initiated because the robot was adjusting the pose of its arm (in order to prevent unnecessary motions of the robot arm, $\dot{\boldsymbol{\theta}}_R$ was zeroed out during all the time that the human arm was outside the robot's workspace). Once their desired relative configuration was achieved, between four and five seconds, the FES signal was sent to the human forearm in order to open the hand. Because the agents achieved good enough coordination, complete success was obtained.

5.4. Both agents perform autonomous movements: the task of pouring water

In the task of pouring water, the robot had to pour the water while the subject held the glass. The task $\underline{\boldsymbol{x}}_{\text{task}\,d} = \boldsymbol{r}_{\text{task}\,d} + \varepsilon(1/2)\boldsymbol{p}_{\text{task}\,d}\boldsymbol{r}_{\text{task}\,d}$ was simply defined as follows: using $\mathcal{F}_R$ as reference (recall Fig. 1), $\boldsymbol{r}_{\text{task}\,d}$ was defined as a rotation of π around x_R—enforcing a face-to-face cooperation—followed by a rotation of $\pi/4$ around z_R. This last rotation was defined to put the robot hand in a

https://doi.org/10.1017/S0263574714000356 Published online by Cambridge University Press

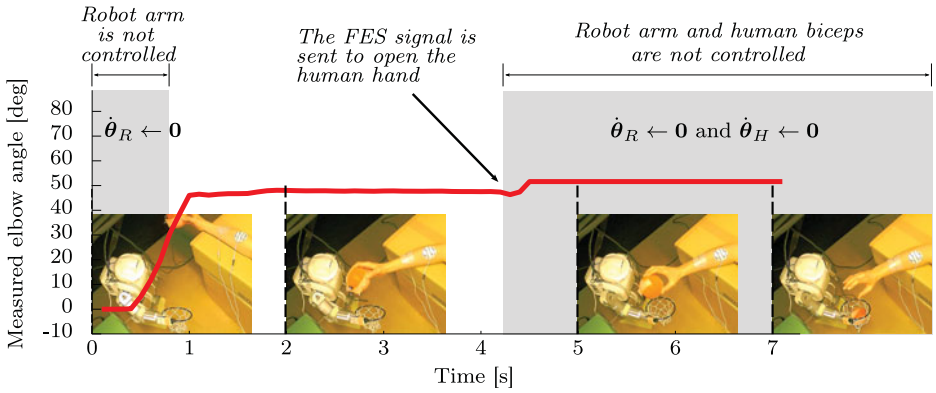

Fig. 9. Measured angle of the human arm for one trial in the ball in the hoop experiment. The gray areas correspond to situations where one or more components of the task joint velocity vector are zeroed out. The pictures are snapshots of the experiment and the left side of each one is aligned with the correspondent snapshot time (*vertical dashed lines*). See provided video #1 for other executions with different subjects.

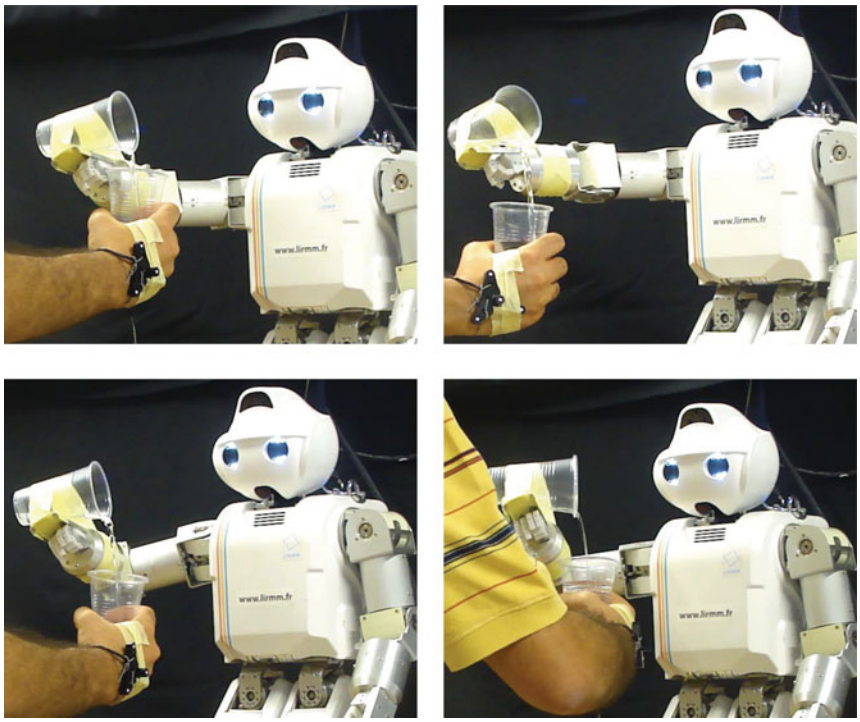

Fig. 10. In the task of pouring water only the robot arm is controlled; thus, $\boldsymbol{J}_{\underline{\boldsymbol{x}}_H^{\mathcal{T}}} \leftarrow 0$ and the control law (8) is equivalent to (9). The four figures correspond to four different spots. See provided video #1 in order to see the reactive behavior of the robot.

pose suitable for pouring water. The corresponding translation $\boldsymbol{p}_{\text{task}\,d}$ was chosen by considering the size of the plastic cup and its placement on the back of the robot hand.

In order to assess the robot's capability to interact effectively with its human partner, the person was told to place his hand in different arbitrary locations, all of them feasible in terms of the robot's geometric limitations. The robot successfully poured the water and was capable of tracking the subject's hand whenever the latter moved. In this way, the robot's reactive motions were capable to provide fluid interactions. Some of the locations are shown in Fig. 10.

In this kind of task, humans have the tendency to regard the robot as an autonomous entity with whom they may ultimately cooperate. Since the latter has several mechanical constraints, sometimes the task can be accomplished only if the person helps the robot. For instance, being aware of these

https://doi.org/10.1017/S0263574714000356 Published online by Cambridge University Press

limitations, people will tend to place the hand where the robot will effectively accomplish the task (or at least where they *believe* that the robot can accomplish it).

6. Discussion and Conclusion

This paper has proposed a novel method to describe the pHRI by means of relative configurations between the human hand and the robot hand. We performed several experiments with healthy subjects and a humanoid robot in order to validate the techniques proposed in the paper. The robot's limited dimensions, as well as its restricted motions, posed a challenge to the design of illustrative cooperative tasks, but the platform provided enough versatility to validate the proposed ideas within the chosen set of experiments. Furthermore, some delays in the experimental set-up, mostly due to the communication between the non-realtime kinematic controller used in the interaction system and the realtime system running on the embedded PC card, decreased the overall system performance. However, even in the presence of those delays, the system worked satisfactorily for our application.

The experiments encompassed situations where both agents behave as autonomous entities, and also situations where one agent holds complete control of the task. In this latter case, we explored both cases where the person holds complete control and the one where the robot controls the human arm by means of FES.

One advantage of representing the cooperative task by using relative configurations is because the control loop is closed at the interaction level, and hence the sensory feedback of both human and robot are used to accomplish the task, as demonstrated in the *simultaneous handling* task. In this task, even if the robot is not equipped with force sensors, *there is* force control thanks to the natural force feedback mechanism present in the human body. In this kind of interaction, the system should be analyzed from a holistic point of view, where every agent provides something beneficial, which thus characterizes the collaboration. Moreover, because this task was defined in terms of the relative configuration between the robot hand and the human hand, but the robot perceived the pose of the human wrist, a compliant behavior could be achieved because the subject exploited the fact that his arm has more DOFs than the robot arm. More specifically, the subject used this redundancy to maintain the desired relative pose between the hands, but changed the arm configuration in order to move the robot, while controlling the internal forces using his natural force feedback. However, most tasks involving forces will still require that the robot be equipped with force controllers in order to achieve good compliant behavior.

One task, the *ball in the hoop*, was performed by using a novel approach in pHRI. In this approach, in addition to controlling its own arm, the robot controls the human arm by means of FES. This has an important implication in assistive robotics, mainly when the robot must assist people with impairments who cannot control their upper limbs: the FES control of the human arm may be used to bring the human arm into the robot's workspace, possibly enhancing the human-robot interaction.

An interesting observation is that the addition of human arm control does not change the definition of the task. In fact, whenever the task is represented by means of relative configurations, there is an invariance with respect to which agents are controlled and even with respect to the controlled DOFs. As a consequence, this invariance may potentially reduce the required amount of work for defining and programming new tasks. Moreover, it can be useful when developing general assistant robots, because the task is defined only once and then the robot can interact with several other agents, regardless of whether these agents are other robots or people. In the case of healthy people, the robot would control only itself. In the case of people suffering from motor disabilities (e.g., quadriplegia) or in physical rehabilitation scenarios, the robot could control the human arm—either completely or partially—if otherwise it would be impossible to accomplish the task; for example, when the robot cannot reach the human hand without controlling the human arm. Of course, this does not mean that the robot would control the subjects' arms against their will. The robot would perform only the low-level control of the human arm, whereas the person would ultimately provide high-level commands (e.g., voice commands) to change or abort the task.

Further works will be focused on the control of more muscles of the human arm, and also in the application of the proposed techniques to the assistance and rehabilitation of disabled individuals. Furthermore, considering that humans often co-contracts their muscles only when there are interaction forces between the body and the environment, we did not take into account the effect of co-contraction because we defined the pHRI in terms of kinematic tasks. However, we intend to exploit this effect

in order to extend our framework to situations involving contacts between human and environment or situations that require, for instance, increased stiffness of the human arm. In addition, we plan to integrate our techniques with whole-body motion frameworks[32–35], where the cooperative task would be first defined by using (3), and then the robot would continuously perform a whole-body motion in order to achieve the desired relative configuration between the human hand and the robot hand. Last, we are going to put some effort on the definition of human-robot interactive tasks that involve several subtasks; in this way, the robot will have to automatically switch between these subtasks in order to provide intuitive and natural interactions.

Funding

This work is supported by Agence Nationale de la Recherche (ANR) under grant ANR 07-ROBO-011 in the context of the ASSIST project.

Acknowledgment

The authors thank Christine Azevedo Coste, Mariana Costa Bernardes and Pedro Moreira for participating in the *ball in the hoop* experiment.

References

1. S. S. Groothuis, S. Stramigioli and R. Carloni, "Lending a helping hand: Toward novel assistive robotic arms," *IEEE Robot. Autom. Mag.* **20**(1), 20–29 (Mar. 2013).
2. A. De Santis, B. Siciliano, A. De Luca and A. Bicchi, "An atlas of physical human-robot interaction," *Mech. Mach. Theory* **43**(3), 253–270 (Mar. 2008).
3. M. A. Goodrich and A. C. Schultz, "Human-robot interaction: A survey," *Found. Trends Hum.-Comput. Interact.* **1**(3), 203–275 (2007).
4. H. A. Yanco and J. Drury, "Classifying Human-Robot Interaction: An Updated Taxonomy," *IEEE International Conference on Systems, Man and Cybernetics (IEEE Cat. No.04CH37583)*, IEEE (2004), pages 2841–2846.
5. T. Takubo, H. Arai, Y. Hayashibara and K. Tanie, "Human-robot cooperative manipulation using a virtual nonholonomic constraint," *Int. J. Robot. Res.* **21**(5-6), 541–553 (May 2002).
6. A. Mortl, M. Lawitzky, A. Kucukyilmaz, M. Sezgin, C. Basdogan and S. Hirche, "The role of roles: Physical cooperation between humans and robots," *Int. J. Robot. Res.* **31**(13), 1656–1674 (Aug. 2012).
7. H. I. Krebs, N. Hogan, M. L. Aisen and B. T. Volpe, "Robot-aided neurorehabilitation," *IEEE Trans. Rehabil. Eng.* **6**(1), 75–87 (Mar. 1998).
8. R. Soyama, S. Ishii and A. Fukase, "Selectable Operating Interfaces of the Meal-Assistance Device "My Spoon," *Rehabilitation* (Z. Bien and D. Stefanov, eds.) (Springer Berlin / Heidelberg, 2004) pp. 155–163.
9. T. L. Chen, M. Ciocarlie, S. Cousins, P. M. Grice, K. Hawkins, C. C. Kemp, D. A. Lazewatsky, A. E. Leeper, A. Paepcke, C. Pantofaru, W. D. Smart and L. Takayama, "Robots for humanity: Using assistive robotics to empower people with disabilities," *IEEE Robot. Autom. Mag.* **20**(1), 30–39 (Mar. 2013).
10. E. Sisbot, L. Marin-Urias, X. Broquère, D. Sidobre and R. Alami, "Synthesizing robot motions adapted to human presence," *Int. J. Soc. Robot.* **2**(3), 329–343 (2010).
11. R. Ueha, H. T. T. Pham, H. Hirai and F. Miyazaki, "A Simple Control Design for Human-Robot Coordination Based on the Knowledge of Dynamical Role Division," *IEEE/RSJ International Conference on Intelligent Robots and Systems, 2009 (IROS 2009)* (2009) pp. 3051–3056.
12. B. V. Adorno, A. P. L. Bo, P. Fraisse and P. Poignet, "Towards a Cooperative Framework for Interactive Manipulation Involving a Human and a Humanoid," *IEEE International Conference on Robotics and Automation*, IEEE (May 2011) pp. 3777–3783.
13. B. V. Adorno, A. P. L. Bo and P. Fraisse, "Interactive Manipulation Between a Human and a Humanoid: When Robots Control Human Arm Motion," *IEEE/RSJ International Conference on Intelligent Robots and Systems*, IEEE (Sep. 2011) pp. 4658–4663.
14. J. M. Selig, *Geometric Fundamentals of Robotics*, 2nd ed. (Springer-Verlag New York Inc., 2005).
15. B. Akyar, "Dual quaternions in spatial kinematics in an algebraic sense," *Turk. J. Math.* **32**(4), 373–391 (2008).
16. B. V. Adorno, Two-arm Manipulation: From Manipulators to Enhanced Human-Robot Collaboration [Contribution à la manipulation à deux bras : des manipulateurs à la collaboration homme-robot] *Ph.D. Thesis* (Université Montpellier 2, 2011).
17. J. M. McCarthy, *Introduction to Theoretical Kinematics* (The MIT Press, Cambridge, MA, 1990) pp. 1–145.
18. B. V. Adorno, P. Fraisse and S. Druon, "Dual Position Control Strategies Using the Cooperative Dual Task-Space Framework," *IEEE/RSJ International Conference on Intelligent Robots and Systems*, IEEE, Taipei (Oct. 2010), pages 3955–3960.

19. M. Uchiyama and P. Dauchez, "A Symmetric Hybrid Position/Force Control Scheme for the Coordination of Two Robots," *Proceedings of the IEEE International Conference on Robotics and Automation*, IEEE Comput. Soc. Press (1988) pp. 350–356.
20. D. Williams and O. Khatib, "The Virtual Linkage: A Model for Internal Forces in Multi-Grasp Manipulation," *Proceedings of the IEEE International Conference on Robotics and Automation*, Vol.1 (1993) pp. 1025–1030.
21. P. Chiacchio, S. Chiaverini and B. Siciliano, "Direct and inverse kinematics for coordinated motion tasks of a two-manipulator system," *J. Dyn. Syst. Meas. Control* **118**(4), 691 (1996).
22. F. Caccavale and M. Uchiyama, *Cooperative Manipulators*, chapter 29 (Springer, 2008) pp. 701–718.
23. F. Caccavale, V. Lippiello, G. Muscio, F. Pierri, F. Ruggiero and L. Villani, "Kinematic Control with Force Feedback for a Redundant Bimanual Manipulation System," *IEEE/RSJ International Conference on Intelligent Robots and Systems*, IEEE (Sep. 2011) pp. 4194–4200.
24. F. Caccavale, V. Lippiello, G. Muscio, F. Pierri, F. Ruggiero and L. Villani, "Grasp planning and parallel control of a redundant dual-arm/hand manipulation system," *Robotica* **31**(07), 1169–1194 (Jul. 2013).
25. H.-L. Pham, V. Perdereau, B. V. Adorno and P. Fraisse, "Position and Orientation Control of Robot Manipulators Using Dual Quaternion Feedback," *IEEE/RSJ International Conference on Intelligent Robots and Systems*, IEEE, Taipei (Oct. 2010) pp. 658–663.
26. S. Chiaverini, "Singularity-robust task-priority redundancy resolution for real-time kinematic control of robot manipulators," *IEEE Trans. Robot. Autom.* **13**(3), 398–410 (Jun. 1997).
27. L. F. C. Figueredo, B. V. Adorno, J. Y. Ishihara and G. A. Borges, "Robust Kinematic Control of Manipulator Robots Using Dual Quaternion Representation," *IEEE International Conference on Robotics and Automation (ICRA)*, IEEE, Karlsruhe (2013) pp. 1941–1947.
28. Bruno Siciliano, Lorenzo Sciavicco, Luigi Villani, and Giuseppe Oriolo. *Robotics: modelling, planning and control*. Springer Verlag, 2009.
29. D. B. Popovic and T. Sinkjaer, *Control of Movement for the Physically Disabled: Control for Rehabilitation Technology* (Springer, London, UK, 2000).
30. A. P. L. Bó, Active Pathological Tremor Compensation on the Upper Limbs using Functional Electrical Stimulation [Compensation active de tremblements pathologiques des membres supérieurs via la stimulation électrique fonctionnelle] *Ph.D. Thesis* (Université Montpellier 2, 2010).
31. O. Stasse, P. Evrard, N. Perrin, N. Mansard and A. Kheddar, "Fast Foot Prints Re-Planning and Motion Generation during Walking in Physical Human-Humanoid Interaction," *Proceedings of the 9th IEEE-RAS International Conference on Humanoid Robots* (Dec. 2009) pp. 284–289.
32. L. Sentis and O. Khatib, "Synthesis of whole-body behaviors through hierarchical control of behavioral primitives," *Int. J. Humanoid Robot.* **2**(4), 505–518 (2005).
33. N. Mansard and F. Chaumette, "Task sequencing for high-level sensor-based control," *IEEE Trans. Robot.* **23**(1), 60–72 (Feb. 2007).
34. N. Mansard, O. Khatib and A. Kheddar, "A unified approach to integrate unilateral constraints in the stack of tasks," *IEEE Trans. Robot.* **25**(3), 670–685 (Jun. 2009).
35. O. Kanoun, F. Lamiraux and P.-B. Wieber, "Kinematic control of redundant manipulators: Generalizing the task-priority framework to inequality task," *IEEE Trans. Robot.* **27**(4), 785–792 (Aug. 2011).

Appendix A. Auxiliary Proofs

This appendix presents some auxiliary mathematical proofs used throughout the text.

Fact 1. For a unit dual quaternion $\underline{\boldsymbol{x}}$, the following equality holds: $\bar{\boldsymbol{H}}\left(\underline{\boldsymbol{x}}^*\right) = \bar{\boldsymbol{H}}\left(\underline{\boldsymbol{x}}\right)^+$.

Proof. Consider the unit dual quaternions $\underline{\boldsymbol{x}}$ and $\underline{\boldsymbol{y}}$, such that

$$\bar{\boldsymbol{H}}\left(\underline{\boldsymbol{x}}\right) \operatorname{vec} \underline{\boldsymbol{y}} = \operatorname{vec}\left(\underline{\boldsymbol{y}}\underline{\boldsymbol{x}}\right).$$

Premultiplying both sides by $\bar{\boldsymbol{H}}\left(\underline{\boldsymbol{x}}^*\right)$ yields

$$\begin{aligned}\bar{\boldsymbol{H}}\left(\underline{\boldsymbol{x}}^*\right)\bar{\boldsymbol{H}}\left(\underline{\boldsymbol{x}}\right)\operatorname{vec}\underline{\boldsymbol{y}} &= \bar{\boldsymbol{H}}\left(\underline{\boldsymbol{x}}^*\right)\operatorname{vec}\left(\underline{\boldsymbol{y}}\underline{\boldsymbol{x}}\right)\\ &= \operatorname{vec}\left(\underline{\boldsymbol{y}}\underline{\boldsymbol{x}}\underline{\boldsymbol{x}}^*\right)\\ &= \operatorname{vec}\underline{\boldsymbol{y}}.\end{aligned}$$

https://doi.org/10.1017/S0263574714000356 Published online by Cambridge University Press

Hence $\bar{\boldsymbol{H}}\left(\underline{\boldsymbol{x}}^*\right)\bar{\boldsymbol{H}}\left(\underline{\boldsymbol{x}}\right)=\boldsymbol{I}$. But, since $\bar{\boldsymbol{H}}\left(\underline{\boldsymbol{x}}\right)$ is always invertible, we conclude that $\bar{\boldsymbol{H}}\left(\underline{\boldsymbol{x}}^*\right)=\bar{\boldsymbol{H}}\left(\underline{\boldsymbol{x}}\right)^{-1}=\bar{\boldsymbol{H}}\left(\underline{\boldsymbol{x}}\right)^{+}$. □

Fact 2. For a unit dual quaternion $\underline{\boldsymbol{x}}$, the following equality holds: $\overset{+}{\boldsymbol{H}}\left(\underline{\boldsymbol{x}}\right)=\overset{+}{\boldsymbol{H}}\left(\underline{\boldsymbol{x}}^*\right)^{+}$.

Proof. The proof is analogous to the one of Fact 1. Consider the unit dual quaternions $\underline{\boldsymbol{x}}$ and $\underline{\boldsymbol{y}}$, such that

$$\overset{+}{\boldsymbol{H}}\left(\underline{\boldsymbol{x}}^*\right)\operatorname{vec}\underline{\boldsymbol{y}}=\operatorname{vec}\left(\underline{\boldsymbol{x}}^*\underline{\boldsymbol{y}}\right).$$

Premultiplying both sides by $\overset{+}{\boldsymbol{H}}\left(\underline{\boldsymbol{x}}\right)$ yields

$$\begin{aligned}\overset{+}{\boldsymbol{H}}\left(\underline{\boldsymbol{x}}\right)\overset{+}{\boldsymbol{H}}\left(\underline{\boldsymbol{x}}^*\right)\operatorname{vec}\underline{\boldsymbol{y}}&=\overset{+}{\boldsymbol{H}}\left(\underline{\boldsymbol{x}}\right)\operatorname{vec}\left(\underline{\boldsymbol{x}}^*\underline{\boldsymbol{y}}\right).\\&=\operatorname{vec}\left(\underline{\boldsymbol{x}}\underline{\boldsymbol{x}}^*\underline{\boldsymbol{y}}\right)\\&=\operatorname{vec}\underline{\boldsymbol{y}}.\end{aligned}$$

Hence $\overset{+}{\boldsymbol{H}}\left(\underline{\boldsymbol{x}}\right)\overset{+}{\boldsymbol{H}}\left(\underline{\boldsymbol{x}}^*\right)=\boldsymbol{I}$. But, since $\overset{+}{\boldsymbol{H}}\left(\underline{\boldsymbol{x}}^*\right)$ is always invertible, we conclude that $\overset{+}{\boldsymbol{H}}\left(\underline{\boldsymbol{x}}\right)=\overset{+}{\boldsymbol{H}}\left(\underline{\boldsymbol{x}}^*\right)^{-1}=\overset{+}{\boldsymbol{H}}\left(\underline{\boldsymbol{x}}^*\right)^{+}$. □

Fact 3. If $\boldsymbol{K}\in\mathbb{R}^{8\times 8}$ is a positive-definite matrix, then $\boldsymbol{K}_1\triangleq\boldsymbol{C}_8\bar{\boldsymbol{H}}\left(\underline{\boldsymbol{x}}^*\right)\boldsymbol{K}\bar{\boldsymbol{H}}\left(\underline{\boldsymbol{x}}\right)\boldsymbol{C}_8$, where $\boldsymbol{C}_8$ is given by (7), is also positive definite.

Proof. Consider $\boldsymbol{D}\triangleq\bar{\boldsymbol{H}}\left(\underline{\boldsymbol{x}}\right)\boldsymbol{C}_8$. Since both $\boldsymbol{C}_8$ and $\bar{\boldsymbol{H}}\left(\underline{\boldsymbol{x}}\right)$ are square and have full rank then $\boldsymbol{D}$ also has full rank. Furthermore, for any column vector $\boldsymbol{u}$, there exists a unique vector $\boldsymbol{v}$ such that $\boldsymbol{D}\boldsymbol{v}=\boldsymbol{u}$ and $\boldsymbol{D}\boldsymbol{v}=\boldsymbol{0}$ if and only if $\boldsymbol{v}=\boldsymbol{0}$. Since $\boldsymbol{K}>0$, then for all non-zero $\boldsymbol{u}$:

$$\begin{aligned}\boldsymbol{u}^T\boldsymbol{K}\boldsymbol{u}&>0\\(\boldsymbol{u}^T\boldsymbol{u})^{-1}\boldsymbol{u}^T\boldsymbol{K}\boldsymbol{u}&>0\\\boldsymbol{u}^{+}\boldsymbol{K}\boldsymbol{u}&>0\\\boldsymbol{v}^{+}\boldsymbol{D}^{+}\boldsymbol{K}\boldsymbol{D}\boldsymbol{v}&>0\\(\boldsymbol{v}^T\boldsymbol{v})^{-1}\boldsymbol{v}^T\boldsymbol{D}^{+}\boldsymbol{K}\boldsymbol{D}\boldsymbol{v}&>0\\\boldsymbol{v}^T\boldsymbol{D}^{+}\boldsymbol{K}\boldsymbol{D}\boldsymbol{v}&>0;\end{aligned}$$

hence, $\boldsymbol{D}^{+}\boldsymbol{K}\boldsymbol{D}>0$. Also,

$$\begin{aligned}\boldsymbol{D}^{+}\boldsymbol{K}\boldsymbol{D}&=\left(\bar{\boldsymbol{H}}\left(\underline{\boldsymbol{x}}\right)\boldsymbol{C}_8\right)^{+}\boldsymbol{K}\bar{\boldsymbol{H}}\left(\underline{\boldsymbol{x}}\right)\boldsymbol{C}_8\\&=\boldsymbol{C}_8\bar{\boldsymbol{H}}\left(\underline{\boldsymbol{x}}^*\right)\boldsymbol{K}\bar{\boldsymbol{H}}\left(\underline{\boldsymbol{x}}\right)\boldsymbol{C}_8\\&=\boldsymbol{K}_1.\end{aligned}$$

Therefore, $\boldsymbol{K}_1>0$. □

https://doi.org/10.1017/S0263574714000356 Published online by Cambridge University Press